Journal of Atmospheric and Solar-Terrestrial Physics 169 (2018) 16–22

Contents lists available at ScienceDirect

Journal of Atmospheric and Solar-Terrestrial Physics

journal homepage: www.elsevier.com/locate/jastp

Study of ionospheric irregularities from Kolhapur (16.4°N, 74.2°E)

A.K. Sharma [a], G.A. Chavan [a,*], H.P. Gaikwad [a], O.B. Gurav [a], D.P. Nade [b], S.S. Nikte [c], R.N. Ghodpage [d], P.T. Patil [d]

[a] *Space and Earth Science Laboratory, Department of Physics, Shivaji University, Kolhapur, India*
[b] *Department of Basic Sciences and Humanities, Sou Sushila Danchand Ghodawat Charitable Trust's, Sanjay Ghodawat Group of Institutions, Atigre, India*
[c] *Department of Basic Sciences and Humanities, Vishveshwarya Technical Campus Patgaon-Miraj, India*
[d] *Medium Frequency Radar, Indian Institute of Geomagnetism, Shivaji University Campus, Kolhapur, India*

ARTICLE INFO

Keywords:
Ionospheric scintillation
Fade rate
Cross-correlation function
Scintillation index

ABSTRACT

The paper reports night time observations of ionospheric irregularities made through amplitude scintillation of 251 MHz signal at Kolhapur (16.4°N, 74.2°E), an equatorial Appleton anomaly region using spaced antenna system. Monthly and night time percentage of occurrence of scintillations, during increasing solar cycle from January 2011 to August 2015, is discussed. The parameters such as-maximum cross-correlation function ($\mathbf{C}_I$), Fade Rate are also studied. The percentage occurrence is observed to be higher in post sunset period and during equinoctial months than in winter and summer months. Scintillation occurrence is observed to be suppressed during increasing solar activity. $\mathbf{C}_I$ shows seasonal changes. Percentage of occurrence of $\mathbf{C}_I \geq 0.5$ decreases with increase in solar activity and fade rate also shows solar activity dependence.

1. Introduction

VHF and UHF waves are important for distant communication and navigation but get scintillated due to the presence of ionospheric electron density fluctuations, also known as equatorial spread F (ESF). ESF have been studied and discussed by many researchers in last few decades using spaced receivers at lower latitude stations (Bhattacharyya et al., 1989; Chen et al., 2008; Wernik et al., 2007). It is well known that the ESFs, produced in post sunset hours, are initiated by Rayleigh-Taylor instability process at the bottom side of the F-region. Equatorial plasma bubble (EPB) in F-region, due to Rayleigh-Taylor instability, are produced in equatorial region and move along magnetic field lines towards the crest of equatorial ionization anomaly (EIA) region (Keskinen et al., 1998). Irregularities produced through the Rayleigh-Taylor instability process have scale sizes from few meters to hundreds of Kilometers. In post sunset hours ESF irregularities start to grow and decay in post midnight time (Banola et al., 2005).

Spaced amplitude scintillation receiver system and Global Positioning System (GPS) have been widely used for the study of scintillations of VHF and UHF signals due to the irregularities in equatorial F-region. The structural variability and dynamics of the irregularities have been extensively studied previously since last few decades using spaced receivers technique (Bhattacharyya et al., 2001, 2003; Briggs, 1984; Singh et al., 2010; Sripathi et al., 2011). Effect of magnetic field variability on irregularities has also been studied extensively by many researchers in Indian equatorial region (Kakad et al., 2012; Kumar and Gwal, 2000; Singh et al., 2004). GPS technique also has been used by many researchers for the study of ionospheric scintillation and Total Electron Content (TEC) variability in Indian equatorial region (Acharya et al., 2007; Das et al., 2010). The fade depth of the VHF signal is observed to be higher in equatorial and polar regions. Therefore, it is interesting to study the VHF scintillations from low latitude station Kolhapur (16.42°N, 74.20°E, 10.6° dip.), India, which comes under EIA region. Similar to solar cycle, magnetic field also affects the ionospheric irregularity. Also, the diurnal, nocturnal and seasonal variations cause the perturbation in zonal drift of the ionospheric irregularities (Fejer, 2011). In the Indian region the occurrence of F region irregularities have been studied by several researchers using Ionosonde (Chandra and Vyas, 2010), total electron content (TEC) (Dashora et al., 2012), VHF radar (Patra et al., 2004; Tiwari et al., 2006) and airglow studies (Ghodpage et al., 2013; Mukherjee, 2003; Sharma et al., 2014; Taori and Sindhya, 2014).

For last few decades ionospheric irregularities have been extensively studied and various methodologies have also been developed for the study of their morphology and dynamics (Basu et al., 1991; Bhattacharyya et al., 2001, 2003; Briggs, 1984; Umeki et al., 1977). These studies show that the large equatorial structures produced in F region are

* Corresponding author.
E-mail address: gangadharchavan2@gmail.com (G.A. Chavan).

https://doi.org/10.1016/j.jastp.2017.12.019
Received 19 June 2016; Received in revised form 18 December 2017; Accepted 25 December 2017
Available online 28 December 2017

due to Rayleigh-Taylor instability. Eastward electric field and steep vertical electron density gradient cause the bottom side plasma, in the equatorial F region, to move upward with $\boldsymbol{E} \times \mathbf{B}/B^2$ drift to fall in the equatorial crest region ($\pm 20^0$) along the magnetic field lines of the Earth. The exact mechanism for the instability generation remains to be developed.

2. Method of data analysis

Regular observations of amplitude scintillation of 251 MHz signal transmitted by UFO2 geostationary satellite (positioned at 71.2°E) were carried out in ascending phase of solar cycle from January 2011 to August 2015. Two identical receivers with eleven element Yagi-Uda antennae spaced ~300 m apart in magnetic east-west direction are used for these observations. This system is installed by Indian Institute of Geomagnetism (IIG), Navi Mumbai, under the scientific collaborative program between Shivaji University, Kolhapur (SUK) and IIG. The ionospheric scintillations are digitally recorded with 20 Hz sampling rate. We have analyzed the data to obtain night time variation of S_4 index, fade rate and cross-correlation for each 3 min interval. The amplitude scintillation data of each 3 min interval has been linearly de-trended to remove the trend in the data interval. The de-trended amplitude scintillation data of two spaced antennae for a 3 min interval on 22nd September 2012 at 0257 LT is as shown in Fig. 1. East (red) and West (blue) time series are the amplitudes (in Volts) recorded with respect to time by two receivers placed magnetically east and west respectively.

Ionosphere causes fluctuation (scintillation) to the radio signals passing through it. These may be the fluctuations in amplitude, phase and frequency of the radio signal. The parameter scintillation index (S_4) is the root mean squared standard deviation of intensity of the signal, in general, indicates the strength of amplitude scintillation (Wernik et al., 2004)

$$S_4^2 = \frac{\langle I^2 \rangle - \langle I \rangle^2}{\langle I \rangle^2}$$

We have calculated the S_4 index for each 3 min interval and to minimize the effect of noise in the signal, we have used only the data intervals having S_4 greater than 0.15 for further analysis. This data interval is considered as an event. For the calculation of percentage of occurrence we have considered the event with all data intervals. The S_4 index can be categorized into three categories as weak ($0.15 \le S_4 < 0.3$), moderate ($0.3 \le S_4 < 0.5$) and strong ($0.5 \le S_4 \le 1$) (Bhattacharyya et al., 2003).

2.1. Fade rate

Fade rate, which is the inverse of autocorrelation interval time, has been calculated for each interval using the autocorrelation function. Autocorrelation interval time for a given interval is the time for which autocorrelation fall to 0.5 of its maximum (Banola et al., 2005).

2.2. Calculation of percentage occurrence

The total numbers of data intervals have been considered in order to calculate monthly and daily percentage of occurrence of scintillation events, cross correlation (all of them may or may not satisfy the S_4 criteria).

2.3. Averaging

For statistical analysis many times it is necessary to find the average of the data series for many parameters. Averaging of the data has done by using following scheme:

1) Monthly average of any parameter with time has been calculated only if we have data of more than five days.
2) Similarly, if we have more than five available days in a month but, at particular time if more than five events have not been occurred then average of data for this time has not been considered in analysis or interpretation.

2.4. Cross correlation function (XCF)

The cross correlation between the two signal gives information about density variation in the ionosphere. The cross correlation can be calculated by space-time intensity correlation function given as,

$$C_I(x,t) = \langle I(x_1,t_1)I(x_2,t_2) \rangle$$

(Bhattacharyya et al., 2003) where, triangular brackets represent the ensemble average, spatial lag $x = x_1 - x_2$ and time lag $t = t_1 - t_2$. In the present technique, it is assumed that the one dimensional space-time correlation function has following the form as,

$$C_I(x,t) = f\left[(x_o - V_o t)^2 + V_c^2 t^2\right]$$

Here f is a monotonically decreasing function of its argument, with $f(0) = 1$, V_0 is the average drift speed of the ground scintillation pattern along the baseline, and the parameter V_c, generally referred to as the random velocity, is a measure of the decorrelation between the signals recorded by the two receivers, due to random changes in the characteristics of the irregularities. The relation for V_0 and V_c can be obtained by applying the boundary conditions on above equation.

The maximum value of cross correlation function $C_I(x,t)$ obtained at time t_m for the two spaced receivers having separation x_o is $C_I(x_o, t_m)$. This is useful for finding correlation between two signals. If it is greater

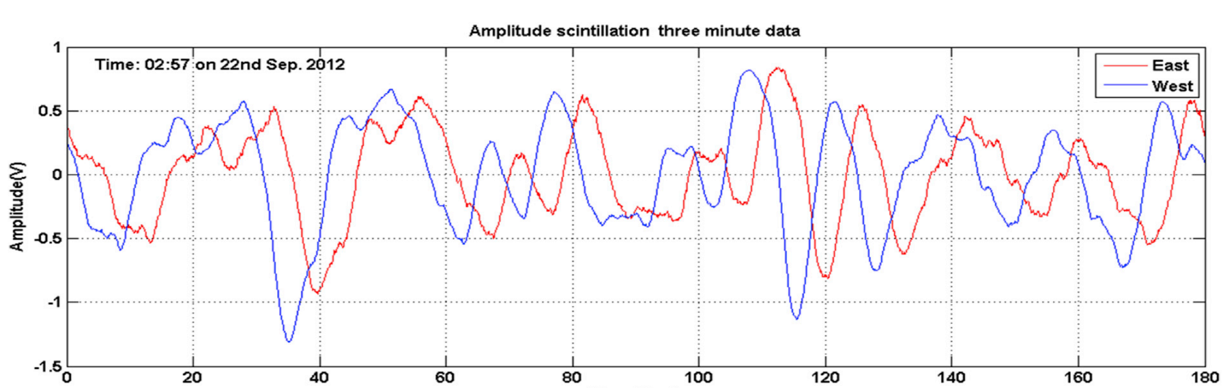

Fig. 1. Amplitude scintillation signal for 3 min duration received by two antennae situated in magnetically east-west direction.

than 0.5 for a data interval then at this time the evolution of irregularity is said to be small and this data interval can be considered for further analysis.

3. Result and discussion

3.1. S_4 Index

To study the ionospheric density fluctuations, it is needed to analyze the parameter, scintillation index (S_4) which gives the information about them through calculation of magnitude of fluctuations of radio waves. Because of prereversal enhancement, F region dynamo and presence of sufficient conditions for the growth of R-T instability, the ionospheric irregularities are formed in the post sunset period (Hunsucker and Hargreaves, 2003; Kelley, 2009). The formation phase may be referred as the generation phase of irregularity in the post-sunset period (Kakad et al., 2007) causes the scintillation of radio signal, therefore the scintillation in this period is strong as observed in Fig. 2. This figure is the monthly averaged S_4 of September 2012 plotted with time. The September is the month of maximum percentage occurrence of 2012. Scintillation index of the post midnight period decreases as in Fig. 2. Table 1 gives monthly pre and post midnight S_4 for all months from January 2011 to August 2015. It is observed that S_4 in pre-midnight period is higher than that in post-midnight period for all months independent on increase in solar flux except for few months in 2015. Higher values of S_4 may be due to generation phase of the irregularities in pre midnight period and decay phase in post midnight period. In few months of 2015, it is observed that S_4 in pre midnight period is less than that in post midnight period. This may be due to the freshly generated irregularities in post midnight period in these months. It should also be noted from table that S_4 for both pre and post-midnight period goes on decreasing with years from January 2011–August 2015.

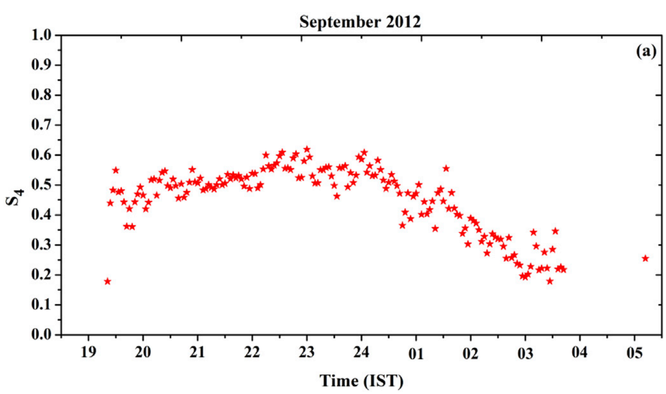

Fig. 2. Monthly averaged night time variation of S_4 for quiet days of September 2012.

Presence of irregularities across the signal path is responsible for occurrence of scintillation event. The strength of scintillation is measured by S_4 index. It is observed that scintillation depends on time, season as well as latitude, longitude and solar activity since, dynamics of the irregularities produced in ionosphere depend on all of these parameters. So, to understand the dependence of scintillation on these parameters, here we have used the S_4 index data. The percentage of occurrence of scintillation for the all available data has calculated for duration from 2011 to August 2015. Monthly variation of scintillation index for categories weak, moderate and strong scintillation indices is given in Fig. 3. In this figure length of bar of each color gives number of counts (events) for each category. Number of counts for strong scintillation is higher for equinoctial period but it decreases with months and it negligibly appears in 2014 and 2015. Number of counts for the moderate scintillation is higher in equinoctial months. Weak scintillations also show higher counts in equinoctial period and near about constant (independent of months and season) occurrence on all other months. Bhattacharyya et al. (2003) found that the occurrence of strong scintillations on an L-band signal requires the presence of small coherence scale lengths in the scintillation pattern. The comparison of coherence scale on quiet and disturbed days shows that strong scintillations are due to the small coherence scales and weak scintillations are due larger coherence scales (Chavan et al., 2016). The decrease in occurrence of strong scintillation may refer to the decrease in scale lengths of irregularities during higher solar activity period.

3.2. Monthly averaged percentage occurrence

Dependence of scintillation on solar activity has been studied earlier by many researchers in Indian region (Kumar and Gwal, 2000; Muella et al., 2009; Pathan and Rao, 1996). In the present paper the amplitude scintillation data has been used from January 2011 to December 2015 which falls within increasing phase of this solar cycle. The 10.7 cm solar flux has been used as the measure of solar activity. To study the effect of solar cycle on monthly averaged percentage of occurrence of the scintillation events, it is plotted with monthly average of 10.7 cm solar flux as in Fig. 4. It can be seen that monthly averaged percentage of occurrence has higher values in initial years and then it is decreased in last two years. In this period, phase of solar cycle is increasing as can be seen from the increasing trend of solar flux. In last two years solar flux is significantly high but percentage of occurrence is less as compared to the previous period. This indicates that the strong solar activity suppresses the scintillation occurrence. This may be due to increase in upward drift after sunset at the time of solar maxima. Fejer et al. (1999) observed that the occurrence of spread F which is associated with the vertical drift decreases with the increase in solar activity. These results are similar to that

Table 1
Monthly pre and post midnight scintillation indices from Jan. 2011 to Aug. 2015.

Year→	2011		2012		2013		2014		2015	
Months ↓	Pre-midnight	Post-midnight	Pre-midnight	Post-midnight	Pre-midnight	Post-midnight	Pre-midnight	Post-midnight	Pre-midnight	Post-midnight
Jan	0.43	0.32	0.48	0.37	0.36	0.33	0.26	0.28	0.33	0.31
Feb	0.57	0.40	0.47	0.33	0.40	0.35	0.28	0.32	0.36	0.43
Mar	0.68	0.46	0.41	0.27	0.45	0.34	*	*	0.39	0.41
Apr	0.66	0.59	0.53	0.47	0.44	0.41	*	*	0.44	0.39
May	*	0.19	0.86	*	0.42	0.39	*	*	0.35	0.27
Jun	*	0.22	0.46	0.16	0.37	0.37	0.28	0.29	*	0.32
Jul	*	*	*	0.38	*	*	*	*	*	*
Aug	0.44	0.50	0.37	0.51	0.62	0.48	0.33	0.28	*	0.19
Sep	0.58	0.50	0.52	0.39	0.65	0.42	0.34	0.33		
Oct	0.74	0.58	0.51	0.41	0.62	0.43	0.51	0.33		
Nov	0.63	0.62	0.47	0.37	0.20	0.40	0.34	0.32		
Dec	0.57	0.48	0.45	0.46	0.27	0.28	0.32	0.27		

*No events found.

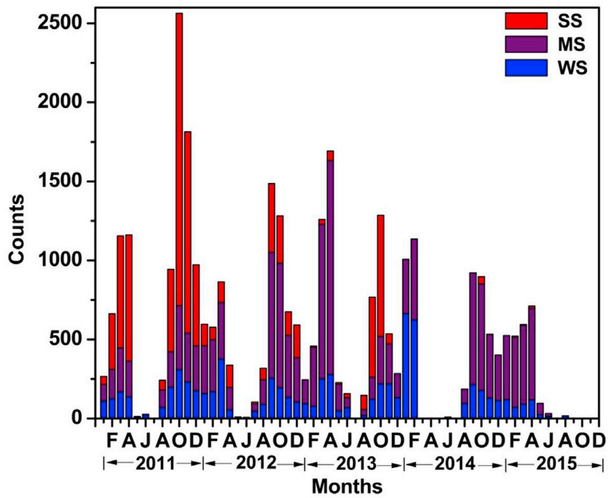

Fig. 3. Number of counts for each month for weak, moderate and strong scintillation are represented by blue, purple and red color respectively. (For interpretation of the references to color in this figure legend, the reader is referred to the Web version of this article.)

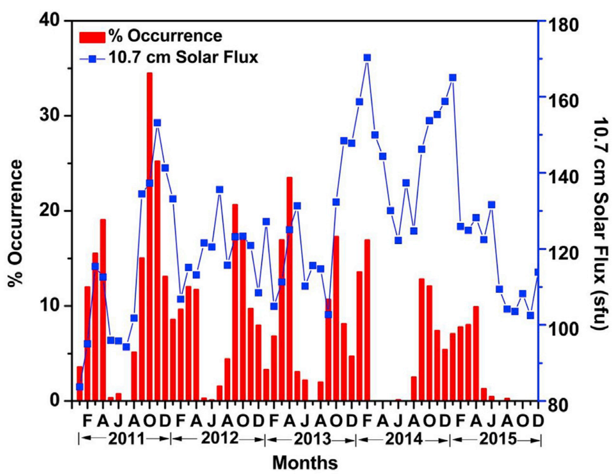

Fig. 4. Monthly percentage occurrence from January 2011 to August 2015 plotted with monthly averaged 10.7 cm solar flux.

of (Singh et al., 2004, 2010) in Indian region. Singh et al. (2010) found that during ascending and descending phase of solar cycle percentage of occurrence scintillation increase and decreases respectively. Many researchers observed that scintillation occurrence varies linearly with solar activity (Chakraborty et al., 1999; Kumar and Gwal, 2000; Rastogi et al., 1981) although we observed the suppression at high solar activity.

3.3. Seasonal percentage of occurrence for each month

To examine the night time scintillation occurrence in each season, the average of monthly percentage of occurrence of scintillation for each season has been taken into account. Seasonal behavior of percentage of occurrence with night time is as shown in Fig. 5. It can be clearly seen that overall occurrence in equinoctial (March–April and September–October) period is higher than the summer (May to August) and winter (January–February and November–December). In post sunset period of equinoctial months the percentage occurrence increases and attains maxima between 21 and 22 LT. The percentage occurrence at this time is 25.75% and then it continues to decrease throughout the remaining night. Similar behavior is observed for winter, but for summer period maxima is observed after midnight at 01 LT. These results agree well with

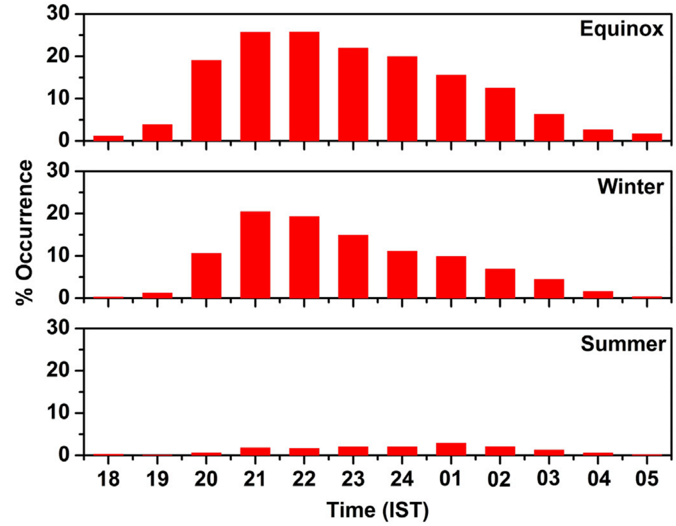

Fig. 5. Averaged seasonal percentage occurrence for the data from January 2011 to August 2015.

the results of seasonal occurrence obtained by Vyas and Dayanandan (2011). They found that in equinoctial and winter season maxima of percentage occurrence observed in between 21 and 22 LT and in summer season maxima of percentage occurrence extend to the post midnight period.

Vyas and Dayanandan (2011) and Valladares et al. (1996) observed higher percentage of occurrence in equinoctial period, moderate in winter and lower in summer, which is similar to the study presented in this paper. Also, these results give the information about the occurrence of irregularities may be useful database at this latitude at the increasing solar cycle. These results occurrence of scintillations may be due to the enhancement in the vertical plasma drift in equinox, winter and reduction in summer months (Lee et al., 2005).

3.4. Fade rate

Depth of fading of the radio signal indicates the degradation of the signal which can be determined by fade rate. This is the useful parameter to see the effect of irregularities on radio signal, therefore to study the variation and behavior of irregularities. The monthly averaged fade rate of September 2012 plotted as the sample with time is shown in Fig. 6. The month September is the month of maximum percentage of occurrence in 2012. The fade rate in pre-midnight period is higher and then decreases with time. This may be due to evolution phase of the irregularities in pre mid night period and decay phase in post mid night period. Monthly averaged fade rate in pre and post-midnight period for each month is determined and shown in Table 2 which shows the higher values in pre-midnight period for each month. Banola et al. (2005) found higher fade

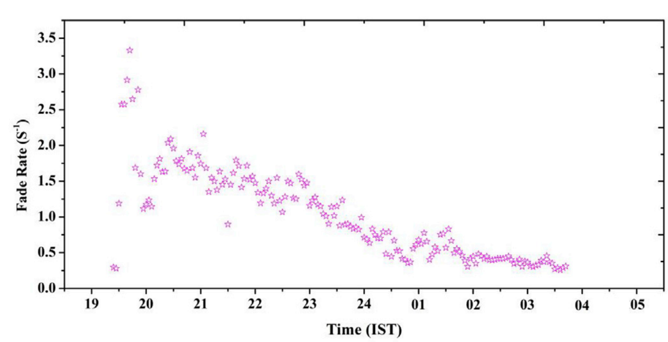

Fig. 6. Monthly averaged fade rate (s^{-1}) for September 2012.

Table 2
Monthly pre and post midnight fade rate from Jan. 2011 to Aug. 2015.

Year→	2011		2012		2013		2014		2015	
Months ↓	Pre-midnight	Post midnight	Pre-midnight	Post midnight	Pre-midnight	Post-midnight	Pre-midnight	Post midnight	Pre-midnight	Post midnight
Jan	*	0.66	1.21	0.71	1.03	0.72	*	*	1.46	0.86
Feb	1.06	0.96	1.28	0.45	1.27	0.56	*	*	1.46	0.90
Mar	1.51	0.53	1.50	0.56	1.47	0.42	*	*	1.49	0.90
Apr	1.65	0.84	1.63	0.73	1.61	0.81	*	*	1.40	0.92
May	*	*	*	*	1.02	0.74	*	*	*	0.91
Jun	*	*	1.03	*	0.29	0.25	*	*	*	*
Jul	*	*	*	0.21	*	*	*	*	*	*
Aug	1.90	0.60	1.38	0.61	1.18	0.60	1.11	0.83	0.33	*
Sep	1.54	0.64	1.42	0.49	1.75	0.72	1.59	0.81		
Oct	1.63	0.75	1.38	0.60	1.48	0.71	1.28	0.85		
Nov	1.69	0.99	1.26	0.49	*	*	1.22	1.26		
Dec	1.22	0.86	1.15	0.81	*	*	1.23	0.8		

*No events found.

rate of the signal in pre midnight period. As well as, the fade rate in post-midnight period decreases from the year 2011–2015. This is may be due to the increase in variability of irregularities and so the fade rate in post-midnight period at the time of higher solar activity.

3.5. *Cross-correlation coefficient (XCF)* $\mathbf{C_I(x,t)}$

The maximum cross correlation $C_I(x_0, t_m)$ [C_I] between two signals can be used as the parameter to study generation and decay phase of the irregularities. When the irregularities in generation phase pass across the signal path, cross correlation C_I between signals received by two antennae decreases to smaller values. Fig. 7 shows that before 2130 LT C_I have smaller values. This is because of the presence of perturbation in electric field associated with irregularities generated in Rayleigh-Taylor instability process in post sunset period. The period for which maximum cross correlation is less than 0.5 is considered as the most affected period (Kakad et al., 2007, 2012). In this period irregularities are said to be evolved randomly. The percentage of occurrence of $C_I \geq 0.5$ and $C_I < 0.5$ for all months in five years is useful in order to study the presence of randomly evolving irregularities. The averaged percentage of occurrence of each month with time for both categories is plotted as contours shown in Fig. 8(a) and (b).

The maximum percentage of occurrence of $C_I \geq 0.5$ for each year is observed to be around 2130 LT and 1–2 h after for all months. The percentage of occurrence of $C_I < 0.5$ for each year is observed to be higher during 1900–2130 LT. This is the indication of generation phase of the irregularities in this period. It should also be noted that in last two years $C_I < 0.5$ shows occurrence in midnight and post midnight period but in initial three years there are no significant events of occurrence of $C_I < 0.5$ in this period, this leads to the fact that the ESF irregularities are generated in midnight and post midnight period in the years of higher solar activity. Moreover $C_I \geq 0.5$ shows decrease in occurrence from 2011 to 2015, this indicates the generation of randomly evolving irregularities in higher solar activity days.

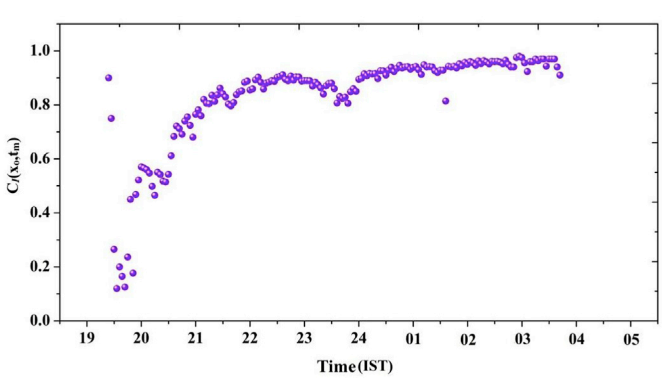

Fig. 7. Monthly averaged cross correlation $C_I(x_o, t_m)$ for September 2012.

4. Summary and conclusions

In this paper, amplitude scintillation data of five year of increasing phase of solar activity (January 2011 to August 2015) has been utilized to study the variation of different parameters of night time ionospheric irregularities using scintillated radio signal. The significant results are summarised below:

1) The nocturnal variation of S_4 shows, higher scintillation in premidnight period and it decreases in postmidnight period in all the five year data independent on solar flux. This is due to the fact that the ESF irregularities are generated in premidnight period and then decay steadily in postmidnight period. Fade rates are also observed to be higher in pre-midnight than in post-midnight for all months. This may also be due to higher variation of the ESF irregularities in the generation phase.
2) All scintillation events are categorized into strong, moderate and weak. Strong scintillation shows higher percentage of occurrence on equinoctial period lower in winter and summer period. Percentage of occurrence of strong scintillations seems to be decreased as increase in solar activity. Comparitively, moderate sintillation increase with solar activity and weak scintillation do not indicate any strong seasonal or solar activity dependence for over all given period. This behavior of strong, moderate and weak scintillations suggests that, with the solar activity, the irregularities causing strong scintillations are suppressed while that of causing moderate or weak scintillations shows small decrease for all months.
3) Monthly percentage of occurrence for all given data is used for the observations of seasonal changes. Maximum percentage of occurrence is observed on equinoctial months lower in summer and moderate in winter period. It is observed that at the time of solar maximum percentage of occurrence of scintillation is small, this suggest that increase in solar activity suppresses the scintillations of the radio signal. This may be due to enhancement of the vertical drift in equinox and winter and reduction in summer season. The depth of fading is also observed to be increased with increasing solar activity.
4) Because of the presence of highly evolving non-frozen irregularities in the premidnight period the correlation between the signal passing through them is very low. Therefore, C_I is lower in premidnight period and goes towards saturation in post midnight period. Observation of C_I at solar maxima shows decrease in occurrence of $C_I \geq 0.5$ and increase in occurrence of $C_I < 0.5$ is the indication of generation of randomly evolving irregularities in this period.

From above discussion it is clear that irregularities generation and

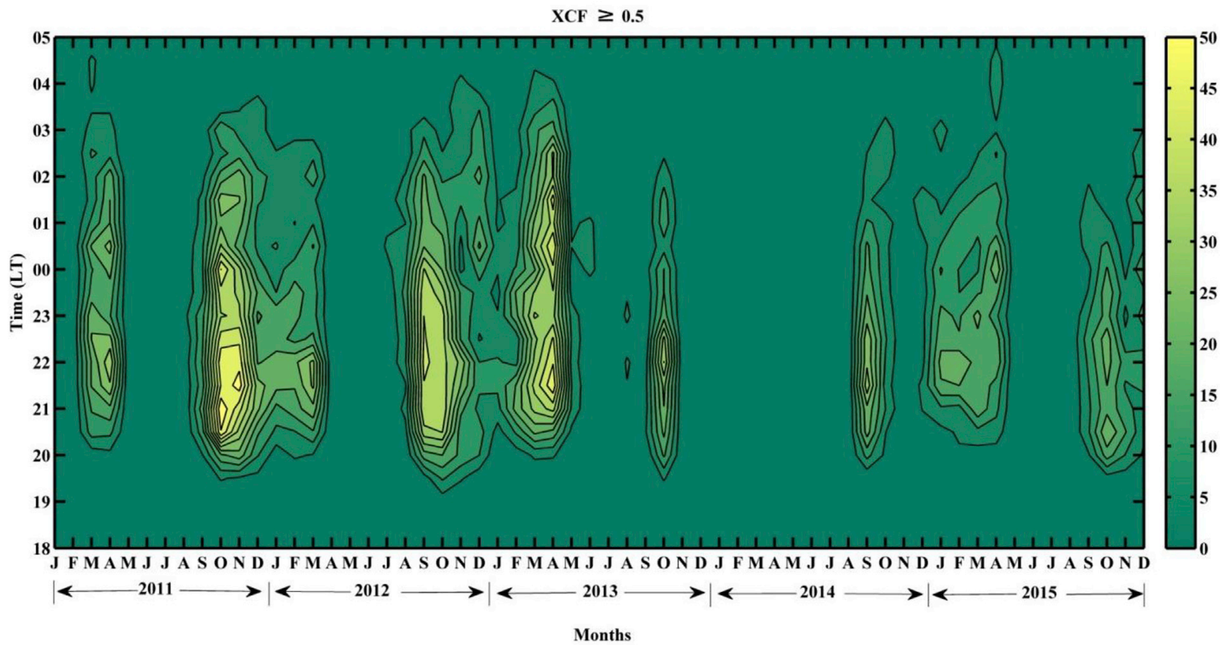

(a)

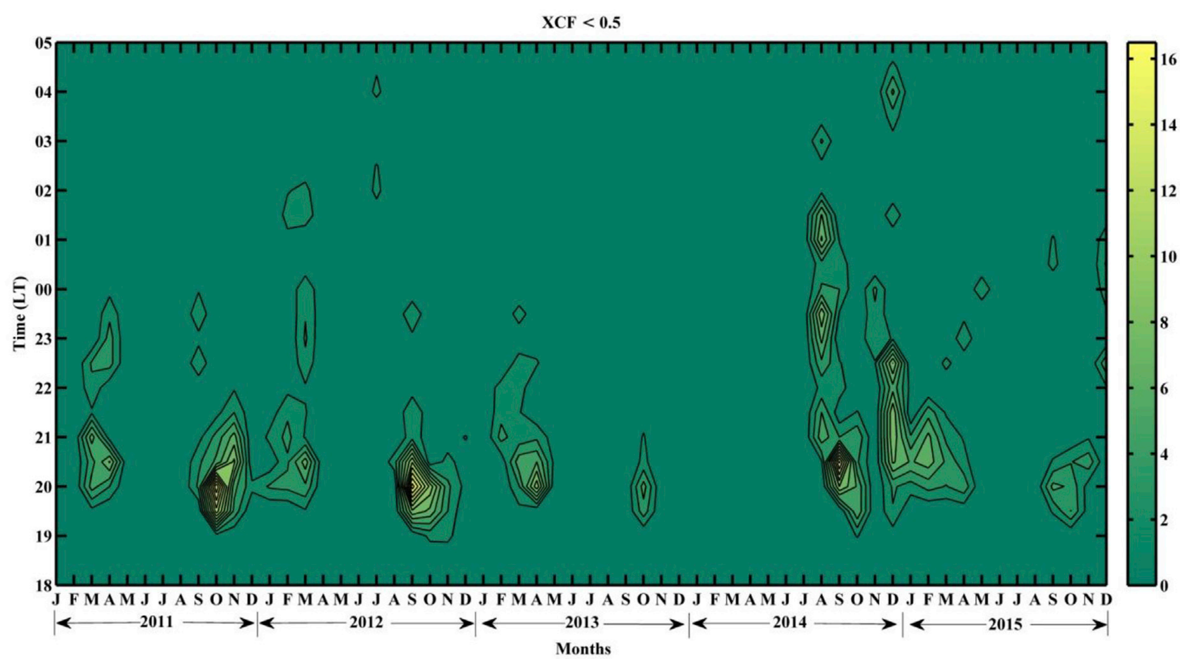

(b)

Fig. 8. (*a*) The % occurrence of maximum cross correlation $C_I \geq 0.5$ for all months from January 2011 to December 2015 (*b*) The % occurrence of maximum cross correlation $C_I < 0.5$ for all months from January 2011 to December 2015.

decay process is independent on solar activity. However, higher occurrence of moderate and weak scintillation is observed in higher solar activity period may be the indication of comparably larger irregularities in this period. So, it will be useful in future to study the scale length variation of irregularities on the basis of solar activity. Increase of post midnight fade rate with solar activity is due to higher variability of these irregularities. This is supported by the cross correlation analysis. The factor responsible for the large variation in the irregularities may be due to vertical electric field which attributes to large eastward velocity. The fade rate shows increase with solar activity in postmidnight but reverse is observed for S_4 which shows independence with each other.

Acknowledgement

The authors are thankful to Indian Institute of Geomagnetism (IIG), Mumbai for providing amplitude scintillation data. One of the authors Mr. G. A. Chavan is thankful to UGC for providing UGC-BSR Junior reseach fellowship and to Dr. Bharati Kakad (IIG) for the scientific

discussion.

References

Acharya, R., Nagori, N., Jain, N., Sunda, S., Regar, S., Sivaraman, M.R., Bandopadhyay, K., 2007. Ionospheric studies for the implementation of GAGAN. Indian J. Radio Space Phys. 36, 394–404.

Banola, S., Pathan, B.M., Rao, D.R.K., Chandra, H., 2005. Spectral characteristics of scintillations producing ionospheric irregularities in the Indian region. Earth Planets Space 57, 47–59.

Basu, S., Basu, S., Kuoeki, E., Zengingonul, H.P., Biondi, M.A., Meriwether, J.W., 1991. Zonal irregularity drifts and neutral winds measured near the magnetic equator in Peru. J. Atmos. Terr. Phys. 53, 743–755. https://doi.org/10.1016/0021-9169(91)90125-Q.

Bhattacharyya, A., Franke, S.J., Yeh, K.C., 1989. Characteristics velocity of equatorial F region irregularities determined from spaced receiver scintillation data. J. Geophys. Res. 94, 11959–11969. https://doi.org/10.1029/JA094iA09p11959.

Bhattacharyya, A., Basu, S., Groves, K.M., 2001. Spaced receiver scintillation observations. Geophys. Res. Lett. 28, 119–122.

Bhattacharyya, A., Groves, K.M., Basu, S., Kuenzler, H., Valladares, C.E., Sheehan, R., 2003. L-band scintillation activity and space-time structure of low-latitude UHF scintillations. Radio Sci. 38, 1–9. https://doi.org/10.1029/2002RS002711.

Briggs, B.H., 1984. The Analysis of Spaced Sensor Records by Correlation Techniques, vol. 13. Middle Atmos. Progr. Handb. MAP, pp. 166–186.

Chakraborty, S.K., DasGupta, A., Ray, S., Banerjee, S., 1999. Long-term observations of VHF scintillation and total electron content near the crest of the equatorial anomaly in the Indian longitude zone. Radio Sci. 34, 241–255. https://doi.org/10.1029/98RS02576.

Chandra, H., Vyas, G.D., 2010. Abnormally low F-layer ionization over Ahmedabad during the night of 26–27 November 1984. Indian J. Radio Space Phys. 39, 346–352.

Chavan, G.A., Sharma, A.K., Gurav, O.B., Gaikwad, H.P., Nade, D.P., Nikte, S.S., Ghodpage, R.N., Patil, P.T., 2016. Dependence of coherence scales of ionospheric scintillation patterns on magnetic activity. MAPAN J. Metrol. Soc. India 32, 1–7. https://doi.org/10.1007/s12647-016-0191-3.

Chen, K.Y., Su, S.Y., Yeh, H.C., Liu, C.H., 2008. Scale analysis of pre- and post-midnight ESF bubbles at storm time and quiet time. Adv. Space Res. 42, 1202–1212. https://doi.org/10.1016/j.asr.2007.07.025.

Das, A., Das Gupta, A., Ray, S., 2010. Characteristics of L-band (1.5GHz) and VHF (244MHz) amplitude scintillations recorded at Kolkata during 1996-2006 and development of models for the occurrence probability of scintillations using neural network. J. Atmos. Sol. Terr. Phys. 72, 685–704. https://doi.org/10.1016/j.jastp.2010.03.010.

Dashora, N., Taori, A., Patra, A.K., 2012. Multi-instrument observations of winter solstice F-region irregularities during the low solar activity. Indian J. Radio Space Phys. 41, 220–232.

Fejer, B.G., 2011. Low latitude ionospheric electrodynamics. Space Sci. Rev. 158, 145–166. https://doi.org/10.1007/s11214-010-9690-7.

Fejer, B.G., Scherliess, L., de Paula, E.R., 1999. Effects of the vertical plasma drift velocity on the generation and evolution of equatorial spread F. J. Geophys. Res. 104, 19859–19870. https://doi.org/10.1029/1999JA900271.

Ghodpage, R.N., Taori, A., Patil, P.T., Gurubaran, S., 2013. Simultaneous mesospheric gravity wave measurements in OH night airglow emission from Gadanki and Kolhapur – Indian low latitudes. Curr. Sci. 104, 98–105.

Hunsucker, R.D., Hargreaves, J.K., 2003. The high-latitude ionosphere and its effects on radio propagation. J. Chem. Inf. Model. https://doi.org/10.1017/CBO9781107415324.004. Cambridge University Press, Cambridge.

Kakad, B., Jeeva, K., Nair, K.U., Bhattacharyya, A., 2007. Magnetic activity linked generation of nighttime equatorial spread F irregularities. J. Geophys. Res. Space Phys. 112, 1–11. https://doi.org/10.1029/2006JA012021.

Kakad, B., Nayak, C.K., Bhattacharyya, A., 2012. Power spectral characteristics of ESF irregularities during magnetically quiet and disturbed days. J. Atmos. Sol. Terr. Phys. 81–82, 41–49. https://doi.org/10.1016/j.jastp.2012.04.008.

Kelley, M.C., 2009. The Earth's Ionosphere, second ed. Acadamic press, New york.

Keskinen, M.J., Ossakow, S.L., Basu, S., Sultan, P.J., 1998. Magnetic-flux-tube-integrated evolution of equatorial ionospheric plasma bubbles. J. Geophys. Res. https://doi.org/10.1029/97JA02192.

Kumar, S., Gwal, A.K., 2000. VHF ionospheric scintillations near the equatorial anomaly crest: solar and magnetic activity effects. J. Atmos. Sol. Terr. Phys. 62, 157–167. https://doi.org/10.1016/S1364-6826(99)00090-5.

Lee, C.C., Liu, J.Y., Reinisch, B.W., Chen, W.S., Chu, F.D., 2005. The effects of the pre-reversal ExB drift, the EIA asymmetry, and magnetic activity on the equatorial spread F during solar maximum. Ann. Geophys. 23, 745–751. https://doi.org/10.5194/angeo-23-745-2005.

Muella, M.T.A.H., de Paula, E.R., Kantor, I.J., Rezende, L.F.C., Smorigo, P.F., 2009. Occurrence and zonal drifts of small-scale ionospheric irregularities over an equatorial station during solar maximum - magnetic quiet and disturbed conditions. Adv. Space Res. 43, 1957–1973. https://doi.org/10.1016/j.asr.2009.03.017.

Mukherjee, G.K., 2003. Studies of equatorial F-region depletions and dynamics using multiple wavelength nightglow imaging. J. Atmos. Sol. Terr. Phys. 65, 379–390. https://doi.org/10.1016/S1364-6826(02)00214-6.

Pathan, B.M., Rao, D.R.K., 1996. Seasonal and solar cycle association of zonal drifts of ionospheric plasma irregularities in the Indian equatorial region. Ann. Geophys. 14, 297–303.

Patra, A.K., Sripathi, S., Sivakumar, V., Rao, P.B., 2004. Statistical characteristics of VHF radar observations of low latitude E-region field-aligned irregularities over Gadanki. J. Atmos. Sol. Terr. Phys. 66, 1615–1626. https://doi.org/10.1016/j.jastp.2004.07.032.

Rastogi, R.G., Mullen, J.P., MacKenzie, E., 1981. Effect of geomagnetic activity on equatorial radio VHF scintillations and spread F. J. Geophys. Res. 86, 3661–3664. https://doi.org/10.1029/JA086iA05p03661.

Sharma, A.K., Nade, D.P., Nikte, S.S., Patil, P.T., Ghodpage, R.N., Vhatkar, R.S., Rokade, M.V., Gurubaran, S., 2014. Occurrence of equatorial plasma bubbles over Kolhapur. Adv. Space Res. 54, 435–442. https://doi.org/10.1016/j.asr.2013.07.018.

Singh, R.P., Patel, R.P., Singh, A.K., 2004. Effect of solar and magnetic activity on VHF scintillations near the equatorial anomaly crest. Ann. Geophys. 22, 2849–2860. https://doi.org/10.5194/angeo-22-2849-2004.

Singh, S.B., Patel, K., Patel, R.P., Singh, A.K., Singh, R.P., 2010. Modeling of VHF scintillation observed at low latitude. J. Phys. Conf. Ser. 208, 1–9. https://doi.org/10.1088/1742-6596/208/1/012065.

Sripathi, S., Kakad, B., Bhattacharyya, A., 2011. Study of equinoctial asymmetry in the Equatorial Spread F (ESF) irregularities over Indian region using multi-instrument observations in the descending phase of solar cycle 23. J. Geophys. Res. Space Phys. 116, 1–12. https://doi.org/10.1029/2011JA016625.

Taori, A., Sindhya, A., 2014. Measurements of equatorial plasma depletion velocity using 630 nm airglow imaging over a low-latitude Indian station. J. Geophys. Res. Space Phys. 119, 396–401. https://doi.org/10.1002/2013JA019465.

Tiwari, D., Engavale, B., Bhattacharyya, A., Devasia, C.V., Pant, T.K., Sridharan, R., 2006. Simultaneous radar and spaced receiver VHF scintillation observations of ESF irregularities. Ann. Geophys. 24, 1419–1427. https://doi.org/10.5194/angeo-24-1419-2006.

Umeki, R., Liu, C.H., Yeh, K.C., Oceanic, N., 1977. Multifrequency studies on ionospheric scintillations. Radio Sci. 12, 311–317.

Valladares, C.E., Sheehan, R., Basu, S., Kuenzler, H., Espinoza, J., 1996. The multi-instrumentedst udieso f equatorialt hermosphere aeronomy scintillation system: climatology of zonal drifts. J. Geophys. Res. 101, 26839–26850.

Vyas, B.M., Dayanandan, B., 2011. Nighttime VHF ionospheric scintillation characteristics near the crest of Appleton anomaly station, Udaipur (24.6°N, 73.7°E). Indian J. Radio Space 40, 191–202.

Wernik, A.W., Alfonsi, L., Materassi, M., 2004. Ionospheric irregularities, scintillation and its effect on systems. Acta Geophys. Pol. 52, 237–249.

Wernik, A.W., Alfonsi, L., Materassi, M., 2007. Scintillation modeling using in situ data. Radio Sci. 42, 1–21. https://doi.org/10.1029/2006RS003512.